Organic Solar Cells. Supramolecular Composites of Porphyrins and Fullerenes Organized by Polypeptide Structures as Light Harvesters

Taku Hasobe,*[,a,b,‡] Kenji Saito,[a] Prashant V. Kamat,*[,b] Vincent Troiani,[c] Hongjin Qiu,[c] Nathalie Solladié,*[,c] Kil Suk Kim,[d] Jong Kang Park,[d] Dongho Kim,*[,d] Francis D'Souza,*[,e] and Shunichi Fukuzumi*[,a]

Receipt/Acceptance Data **[DO NOT ALTER/DELETE THIS TEXT]**
Publication data **[DO NOT ALTER/DELETE THIS TEXT]**
DOI: 10.1039/b000000x [DO NOT ALTER/DELETE THIS TEXT]

We have constructed supramolecular solar cells composed of a series of porphyrin-peptide oligomers [porphyrin functionalized α-polypeptides: $P(H_2P)_n$ or $P(ZnP)_n$ (n = 1, 2, 4, 8, 16)] and fullerene assembled on a nanostructured SnO_2 electrode using an electrophoretic deposition method. Remarkable enhancement in the photoelectrochemical performance as well as the broader photoresponse in the visible and near-infrared regions is seen with increasing the number of porphyrin units in α-polypeptide structures. Formation of supramolecular clusters of porphyrins and fullerenes prepared in acetonitrile/toluene = 3/1 has been confirmed by transmission electron micrograph (TEM) and the absorption spectra. The highly colored composite clusters of porphyrin-peptide oligomers and fullerenes have been assembled as three-dimensional arrays onto nanostructured SnO_2 films using an electrophoretic deposition method. A high power conversion efficiency (η) of ~1.6% and the maximum incident photon-to-photocurrent efficiency (IPCE = 56%) were attained using composite clusters of free base and zinc porphyrin-peptide hexadecamers [$P(H_2P)_{16}$ and $P(ZnP)_{16}$] with fullerenes, respectively. Femtosecond transient absorption and fluorescence measurements of porphyrin-fullerene composite films confirm improved electron-transfer properties with increasing number of porphyrins in a polypeptide unit. The formation of molecular assemblies between porphyrins and fullerenes with a polypeptide structure controls the electron-transfer efficiency in the supramolecular complexes, meeting the criteria required for the efficient light energy conversion.

Introduction

In recent years attention has been drawn to develop inexpensive renewable energy sources. New approaches for the production of efficient and low-cost organic solar cells are necessary for future development of next generation devices.[1-7] Progress is being made in the development of heterojunction organic solar cells, which possess an active layer of a conjugated donor polymer and an acceptor fullerenes. In these polymer blends, efficient photoinduced electron transfer occurs at the donor-acceptor interface, and intimate mixing of donor and acceptor is therefore beneficial for efficient charge separation.[4-7] For efficient transport of the positive charge carriers through the donor phase and of electrons via the acceptor phase to the electrodes, a phase-segregated bicontinuous network is required.

One of the most promising strategies is the development of organic solar cells that mimic natural photosynthesis. In the natural photosynthetic system, the light-harvesting complexes are composed of chlorophylls (or bacteriochlorophylls) assembled in protein matrices that absorb light over a wide spectral range.[8-10] The subsequent electron-transfer process in the reaction center is found to occur very rapidly from the special pair toward the quinones to produce the final charge-separated state which has a long lifetime (ca. 1 s) with nearly 100% quantum yield.[11] Thus, light energy conversion of natural photosynthetic system based on the supramolecular assembly in the protein matrix provides us an important information to construct artificial energy conversion systems.[8a]

The first candidate of such components is a porphyrin that is involved in a number of important biological electron transfer systems including the primary photochemical reactions of chlorophylls (porphyrin derivatives) in the photosynthetic reaction centers. Porphyrins contain an extensively conjugated two-dimensional π-system and thus are suitable for efficient electron-transfer. The uptake or release of electrons results in

[a] *Department of Material and Life Science, Division of Advanced Science and Biotechnology, Graduate School of Engineering, Osaka University, SORST, Japan Science and Technology Agency (JST), Suita, Osaka 565-0871, Japan*
E-mail: fukuzumi@chem.eng.osaka-u.ac.jp
[b] *Radiation Laboratory and Departments of Chemistry & Biochemistry and Chemical & Biomolecular Engineering, University of Notre Dame, Notre Dame, Indiana 46556, U.S.A.*
E-mail: pkamat@nd.edu
[c] *Groupe de Synthèse de Systèmes Porphyriniques, G2SP Laboratoire de Chimie de Coordination du CNRS, UPR 8241, 205 route de Narbonne, 31077 Toulouse Cedex 4, France*
E-mail: solladie@lcc-toulouse.fr
[d] *Center for Ultrafast Optical Characteristics Control, Department of Chemistry, Yonsei University, Seoul 120-749, Korea*
E-mail: dongho@yonsei.ac.kr
[e] *Department of Chemistry, Wichita State University, 1845 Fairmount, Wichita, Kansas 67260-0051, U.S.A.*
E-mail: Francis.DSouza@wichita.edu
† Electronic Supplementary Information (ESI) available: photocurrent and photovoltage response of the OTE/SnO_2/$(P(H_2P)_8+C_{60})_m$ electrode, and transient absorption spectra of $(P(H_2P)_1+C_{60})_m$. See http://dx.doi.org/10.1039/b000000x/
‡ Current address: School of Materials Science, Japan Advanced Institute of Science and Technology (JAIST), Nomi, Ishikawa, 923-1292, Japan

minimal structural and solvation change upon electron transfer, resulting in a small reorganization energy of electron transfer.[12] In addition, rich and extensive absorption features of porphyrinoid systems guarantees increased absorption cross-sections and an efficient use of the solar spectrum.[13] The challenge of creating artificial mimics of these light-harvesting complexes has stimulated the development of routes to a diverse collection of multi-porphyrin arrays.[14] In the natural system, bacteriochlorophylls are held by α-helical polypeptides.[15] In this context, we have recently reported synthesis of porphyrin oligomers with polypeptidic backbone in which porphyrins are held in a favored spacing and orientation by fairly short helical polypeptides.[16]

With regard to electron acceptors, fullerene, which is an extensively conjugated three-dimensional π system, is an ideal electron acceptor because of the minimal changes of structure and solvation associated with the electron-transfer reduction.[17] Thus, combination of porphyrin and fullerene is regarded as an ideal donor-acceptor couple, since the combination results in a small reorganization energy, which allows to accelerate photoinduced electron transfer and to slow down charge recombination, leading to the generation of a long-lived charge-separated state with a high quantum yield.[17-22] Combination of porphyrins and fullerenes is also known to form supramolecular complexes, which contain closest contacts between one of the electron-rich 6:6 bonds of the guest fullerene and the geometric center of the host porphyrin.[23-26] The porphyrin-fullerene interaction energies are reported to be in the range from -16 to -18 kcal mol^{-1}.[27] Such a strong interaction between porphyrins and fullerenes is likely to be a good driving force for the formation of supramolecular complexes between porphyrin and fullerene. The association constants also depend on the type of metal ion in a porphyrin ring,[24c] and the differences may make it possible to control electron transport property, which is essential for the photoenergy conversion.

We report herein construction of a organic solar cell composed of porphyrin-peptide oligomers and fullerenes which are prepared by clusterization on SnO_2 electrodes (Scheme 1).[28] We have investigated the effects of the number of porphyrins in a poly-peptide unit [$P(H_2P)_n$ (n = 1, 2, 4, 8, 16) and $P(ZnP)_n$ (n = 1, 2, 4, 8, 16)] and of the types of porphyrins (H_2P *vs.* ZnP) and fullerenes (C_{60} *vs.* C_{60} derivatives) in Fig. 1 on the structures, spectroscopic, and photoelectrochemical properties of the porphyrin-C_{60} composite electrodes. In addition to the photoelectrochemical measurement, the detail structural and photophysical informations between porphyrin and fullerene using circular dichroism (CD), associate constant based on absorption and fluorescence changes, fluorescence lifetime and femtosecond transient absorption spectroscopy are also discussed here.

Scheme 1 Supramolecular organization between porphyrins and fullerenes with a polypeptide structure in this study.

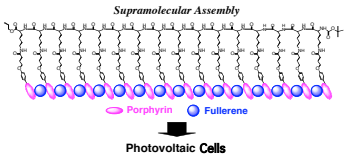

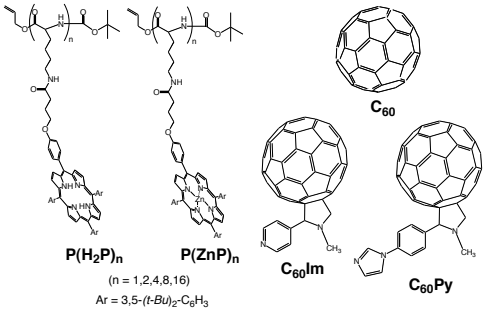

Fig. 1 Porphyrin-peptide oligomers and fullerene derivatives employed in this study.

Experimental

Materials. All solvents and chemicals were of reagent grade quality, obtained commercially and used without further purification unless otherwise noted (*vide infra*). The details of synthesis of porphyrin-peptide oligomers have been reported previously.[16] Nanostructured SnO_2 films were cast on an optically transparent electrode (OTE) by applying a 2% colloidal solution obtained from Alfa Chemicals. The air-dried films were annealed at 673 K. The details of the preparation of SnO_2 films on conducting glass substrate were reported elsewhere.[29] The nanostructured SnO_2 film electrode is referred as OTE/SnO_2.

Electrophoretic deposition of cluster films. A known amount of porphyrin derivatives, C_{60} or mixed cluster solution in acetonitrile/toluene (3/1, v/v, 2 mL) was transferred to a 1 cm cuvette in which two electrodes (viz., OTE/SnO_2 and OTE) were kept at a distance of 6 mm using a Teflon spacer. A DC voltage (300 V) was applied between these two electrodes using a Fluke 415 power supply.[30,31] The deposition of the film can be visibly seen as the solution becomes colorless with simultaneous brown coloration of the OTE/SnO_2 electrode. The OTE/SnO_2 electrode coated with mixed $P(H_2P)_n$ [or $P(ZnP)_n$] and C_{60} clusters is referred to $(P(H_2P)_n+C_{60})_m$ or $(P(ZnP)_n+C_{60})_m$ for simplicity.

The UV-visible spectra were recorded on a Shimadzu 3101 spectrophotometer. Transmission electron micrographs (TEM) of composite clusters of porphyrin and fullerene were recorded by applying a drop of the sample to carbon-coated copper grid. Images were recorded using a Hitachi H600 transmission electron microscope. The morphology of the mesoporous electrodes was characterized by a scanning electron micrograph (SEM; JEOL, JSM-6700FE). The SEM was operated with an accelerating voltage of 10 kV.

Photoelectrochemical measurements. Photoelectrochemical measurements were carried out in a standard two-compartment cell consisting of a working electrode and a Pt wire gauze counter. A Princeton Applied Research (PAR) model 173 potentiostat and Model 175 universal programmer were used for recording *I-V* characteristics. All other photoelectrochemical measurements were carried out using a working electrode and a Pt gauge counter electrode in the same cell assembly using a Keithley model 617 programmable electrometer. The electrolyte was 0.5 M NaI and 0.01 M I_2 in acetonitrile. A collimated light beam from a 150 W Xenon lamp with a 400 nm cut-off filter was used for excitation of $(P(H_2P)_n+C_{60})_m$ [or $(P(ZnP)_n+C_{60})_m$] films

deposited on SnO_2 electrodes. A Bausch and Lomb high intensity grating monochromator was introduced into the path of the excitation beam for the selected wavelength.

Photodynamics measurements. Quenching experiments of the fluorescence of composite films was carried out on a SHIMADZU spectrofluorophotometer (RF-5000). Fluorescence decays were measured by using femtosecond pulse laser excitation and a single photon counting system for fluorescence decay measurements.[31] The laser system was a cavity-dumped femtosecond Ti: Sa laser pumped by a cw Nd:YAG laser (Spectra-Physics, Millenia). The full width at half-maximum of the instrument response function was 53 ps. The fluorescence decays were measured with magic angle emission polarization.

ESR measurements. A quartz ESR tube (internal diameter: 4.5 mm) containing a deaerated acetonitrile/toluene (3/1, v/v) solution of $(P(ZnP)_{16}+C_{60})_m$ was irradiated in the cavity of the ESR spectrometer with the focused light of a 1000-W high-pressure Hg lamp (Ushio-USH1005D) through an aqueous filter at low temperature. The ESR spectra in frozen acetonitrile/toluene were measured under nonsaturating microwave power conditions using a JEOL X-band spectrometer (JES-RE1XE) with an attached variable temperature apparatus. The magnitude of modulation was chosen to optimize the resolution and the signal-to-noise (S/N) ratio of the observed spectra when the maximum slope linewidth (ΔH_{msl}) of the ESR signals was unchanged with a larger modulation magnitude. The *g* values were calibrated with an Mn^{2+} marker.

Femtosecond laser flash photolysis. Ultrafast transient absorption spectroscopy experiments were conducted using Clark-MXR 2010 laser system and an optical detection system provided by Ultrafast Systems (*Helios*). The source for the pump and probe pulses were derived from the fundamental output of Clark laser system (775 nm, 1 mJ/pulse and fwhm = 150 fs) at a repetition rate of 1 kHz. A second harmonic generator introduced in the path of the laser beam provided 387 nm laser pulses for excitation. 95% of the fundamental output of the laser (775 nm) was used to generate the second harmonic, while 5% of the deflected output was used for white light generation. Prior to generating the probe continuum, the laser pulse was fed to a delay line that provided an experimental time window of 1.6 ns with a maximum step resolution of 7 fs. The pump beam was attenuated at 5 μJ/pulse with a spot size of 2 mm diameter at the sample cell where it was merged with the white probe pulse in a close angle (< 10º). The probe beam after passing through the 2 mm sample cell was focused on a 200 μm fiber optic cable which was connected to a CCD spectrograph (Ocean Optics, S2000-UV-vis) for recording the time-resolved spectra (425-800 nm). Typically, 5000 excitation pulses were averaged to obtain the transient spectrum at a set delay time. Kinetic traces at appropriate wavelengths were assembled from the time-resolved spectral data. All measurements were conducted at room temperature, 295 K. When necessary a flow cell was used to circulate the solution through the sample cell.

Results and Discussion

Molecular assembly of porphyrin-peptide oligomers and C_{60} in mixed solvents. Porphyrin-peptide oligomers $[P(H_2P)_n$ or $P(ZnP)_n]$ form supramolecular complexes with fullerene molecules in toluene. In an acetonitrile/toluene mixed solvent system these supramolecular complexes aggregate to form clusters of diameter 100-200 nm. These clusters can be assembled on nanostructured SnO_2 electrodes by an electrophoretic deposition method (500 V/cm for 1 minute) using the methodology described previously.[30] The organization of porphyrin-peptide oligomers and C_{60} composite clusters [denoted as $(P(H_2P)_n+C_{60})_m$ or $(P(ZnP)_n+C_{60})_m$ (n = 1, 2, 4, 8, 16)] was performed by fast injecting a mixed toluene solution of $P(H_2P)_n$ $[P(ZnP)_n]$ and C_{60} into acetonitrile/toluene (3/1, v/v). Herein the concentration of one porphyrin unit in these composite clusters is taken as the same in the oligomers: $[P(H_2P)_1] = [P(ZnP)_1] = 0.19$ mM, $[P(H_2P)_2] = [P(ZnP)_2] = 0.10$ mM, $[P(H_2P)_4] = [P(ZnP)_4] = 0.048$ mM, $[P(H_2P)_8] = [P(ZnP)_8] = 0.024$ mM and $[P(H_2P)_{16}] = [P(ZnP)_{16}] = 0.012$ mM in acetonitrile/toluene (3/1, v/v), whereas the concentration of C_{60} (0.31 mM) is in excess of the concentration of one-porphyrin unit in acetonitrile/toluene (3/1, v/v). This procedure allows us to achieve the supramolecular complex formation between porphyrin-peptide oligomers and C_{60}, and the clusterization at the same time.

Fig. 2 shows the transmission electron micrograph (TEM) images of the composite clusters [A: $(P(H_2P)_{16}+C_{60})_m$, B: $(P(ZnP)_{16}+C_{60})_m$, C: $(P(ZnP)_8+C_{60})_m$ and D: $(P(ZnP)_1+C_{60})_m$]. As solvents evaporate on the copper grid, the clusters form well-defined shapes and sizes. Judging from the molecular scale of porphyrin and C_{60}, one can conclude that porphyrin molecules are self-assembled with C_{60} molecules in the mixed solution to yield large donor-acceptor (D-A) nanoclusters with an interpenetrating network. Especially, in the case of the composite assemblies of porphyrin-peptide oligomers and C_{60} (Fig. 2A-C), the sizes and shapes are much controlled as compared with those of $(P(ZnP)_1+C_{60})_m$ (Fig. 2D). This demonstrates that the size and shapes are largely dependent on the structures of multi-porphyrin arrays.

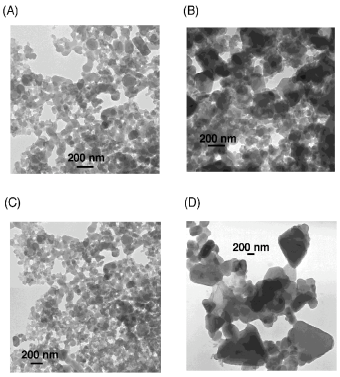

Fig. 2 TEM images of (A) $(P(H_2P)_{16}+C_{60})_m$, (B) $(P(ZnP)_{16}+C_{60})_m$ (C) $(P(ZnP)_8+C_{60})_m$, and (D) $(P(ZnP)_1+C_{60})_m$ composite clusters.

We have also measured absorption spectra of the composite clusters as shown in Fig. 3. The absorption spectra of $(P(ZnP)_n+C_{60})_m$ (spectra a-c) in acetonitrile/toluene 3:1 mixture become broad and red-shifted as compared with those of monomeric form in toluene (spectra d and e). This trend is

enhanced with increasing the number of porphyrins in a polypeptide unit, when the Soret band in $(P(ZnP)_{16}+C_{60})_m$ is red-shifted and the spectrum becomes broad as compared with those of $(P(ZnP)_1+C_{60})_m$ and $(P(ZnP)_2+C_{60})_m$. The broad absorption in the visible and near IR regions is characteristic of π-complexes formed between porphyrins and fullerenes.[32,33] The broader spectrum of $(P(ZnP)_{16}+C_{60})_m$ as compared to that of $(P(ZnP)_1+C_{60})_m$ results from the charge-transfer (CT) type interaction of the π-complex between porphyrin and C_{60} in the long-wavelength absorption of the composite clusters. Similar CT interactions leading to an extended absorption have been observed for porphyrin-C_{60} dyads linked at close proximity.[32-35] In the case of porphyrin-fullerene composite clusters, the higher CT absorption is clearly observed because of the strong interaction, although the scattering effect is also observed.[28,31]

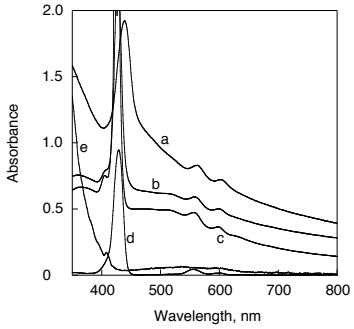

Fig. 3 Absorption spectra of (a) $(P(ZnP)_{16}+C_{60})_m$ ($[P(ZnP)_{16}]$ = 0.012 mM, $[C_{60}]$ = 0.31 mM) in acetonitrile/toluene = 3/1, (b) $(P(ZnP)_2+C_{60})_m$ ($[P(ZnP)_2]$ = 0.10 mM, $[C_{60}]$ = 0.31 mM) in acetonitrile/toluene = 3/1, (c) $(P(ZnP)_1+C_{60})_m$ ($[P(ZnP)_1]$ = 0.19 mM, $[C_{60}]$ = 0.31 mM) in acetonitrile/toluene = 3/1, (d) $P(ZnP)_{16}$ ($[P(ZnP)_{16}]$ = 5 μM) in toluene and (e) C_{60} ($[C_{60}]$ = 150 μM) in toluene.

Association constant between porphyrins and fullerenes. The UV-vis absorption and fluorescence spectral changes give us useful information of supramolecular formation between porphyrins and fullerenes as shown in Fig. 4. The Soret band of $P(H_2P)_{16}$ in benzonitrile at 298 K is red-shifted with clean isosbestic point by addition of C_{60}, and the absorbance change exhibits saturation behavior with increasing C_{60} concentration (Fig. 4A and B). This indicates that C_{60} forms 1:1 complex with the porphyrin moiety of $P(H_2P)_{16}$ as shown in Equation (1), where H_2P is one porphyrin unit in $P(H_2P)_{16}$. According to Equation (1),

$$H_2P + C_{60} \underset{}{\overset{K}{\rightleftharpoons}} H_2P \cdots C_{60} \qquad (1)$$

the K value in Equation (1) can be calculated from Equation (2),[36]

$$[H_2P]_0/(A_0-A) = (\varepsilon_c - \varepsilon_p)^{-1} + (K[C_{60}]\,(\varepsilon_c - \varepsilon_p))^{-1} \qquad (2)$$

where A_0 and A are the absorbance of H_2P at the given wavelength in the absence and presence of C_{60}, and ε_p and ε_c are the molar absorption coefficient of H_2P at the given wavelength in the absence and presence of C_{60}, respectively. The formation constant between $P(H_2P)_{16}$ and C_{60} in benzonitrile is determined as 1.4 x 10^4 M^{-1} from the slope of the plot in the inset of Fig. 4B.

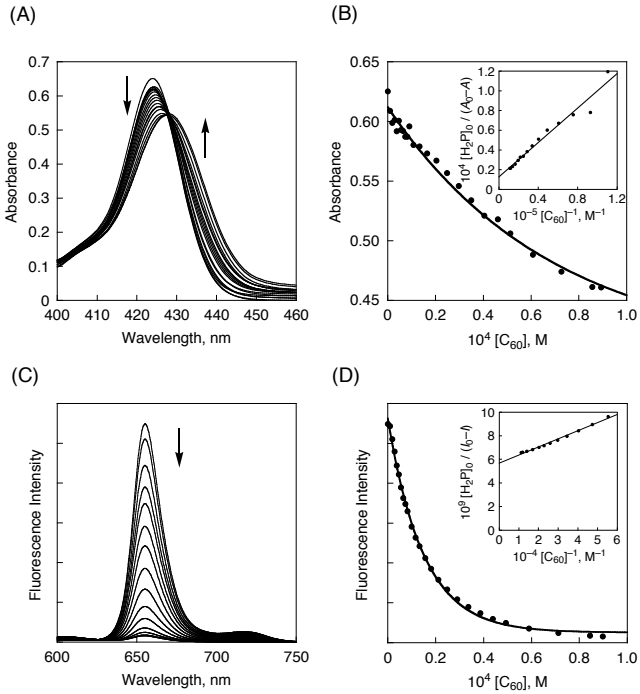

Fig. 4 (A) Absorption spectral changes of $P(H_2P)_{16}$ (3.5 x 10^{-6} M based on one porphyrin unit) in the presence of various concentrations of C_{60} (0 to 8.9 x 10^{-5} M) in PhCN at 298 K. (B) Plot of absorbance at 422 nm *vs.* $[C_{60}]$. Inset: Plot of $[C_{60}]^{-1}$ *vs.* $[H_2P] / (A_0–A)$. (C) Fluorescence spectra of $P(H_2P)_{16}$ (3.5 x 10^{-6} M based on the number of porphyrin unit) in the presence of various concentrations of C_{60} (0 to 9.0 x 10^{-5} M) in deaerated PhCN at 298 K. (D) Change in the fluorescence intensity at 655 nm. Inset: Plot of $[C_{60}]^{-1}$ *vs.* $[H_2P] / (I_0–I)$.

As $P(H_2P)_{16}$ forms the supramolecular complex with C_{60}, the fluorescence of $P(H_2P)_{16}$ may be quenched by intracomplex electron transfer from the singlet excited state of the porphyrin moiety to C_{60}. The apparent formation constant determined from the fluorescence quenching (8.2 x 10^4 M^{-1}) is significantly larger than that determined from the UV-vis spectral change. This indicates that the excited energy migration between the porphyrin units occurs efficiently prior to the electron transfer. The K values of various types of porphyrin-peptide oligomers $[P(H_2P)_n$ or $P(ZnP)_n]$ and C_{60} derivatives are listed in Table 1. The association constant between porphyrins and C_{60} increases with increasing number of porphyrins in a polypeptide unit. This indicates that the interaction between porphyrin and C_{60} becomes stronger with increasing the number of porphyrins in the porphyrinic polypeptide. The large association constant in $P(H_2P)_n$–C_{60} system relative to $P(ZnP)_n$–C_{60} system indicates that free base porphyrins in the polypeptidic structure can accommodate C_{60} molecules between two porphyrin rings more easily than zinc porphyrins as reported for the complex formation between a porphyrin and fullerene.[31] When C_{60} is replaced by C_{60} derivatives bearing either imidazole and pyridine coordinating ligands (C_{60}Im and C_{60}Py), the association constants in $P(ZnP)_{16}$–C_{60}Im and $P(ZnP)_{16}$–C_{60}Py systems become much larger than that of $P(ZnP)_{16}$–C_{60} system due to the π-π interaction between porphyrins and fullerenes *plus* axial coordination to zinc porphyrin in $P(ZnP)_{16}$. Such differences in the association constants certainly affect the light energy conversion efficiencies (*vide infra*).

Table 1. Comparison of the binding constants between porphyrins and C_{60}

Fullerene	Porphyrin	*K*, M^{-1}		Porphyrin	*K*, M^{-1}	
		UV-vis	Fluorescence		UV-vis	Fluorescence
C_{60}	$P(ZnP)_2$	—	—	$P(H_2P)_2$	—	—
C_{60}	$P(ZnP)_4$	5.9×10^2	5.0×10^3	$P(H_2P)_4$	2.7×10^3	9.5×10^3
C_{60}	$P(ZnP)_8$	4.1×10^3	1.4×10^4	$P(H_2P)_8$	5.3×10^3	2.2×10^4
C_{60}	$P(ZnP)_{16}$	6.7×10^3	3.9×10^4	$P(H_2P)_{16}$	1.4×10^4	8.2×10^4
C_{60}Im	$P(ZnP)_{16}$	5.8×10^4	7.9×10^6			
C_{60}py	$P(ZnP)_{16}$	3.7×10^4	8.3×10^5			

Circular dichroism (CD) measurement. We have measured the circular dichroism (CD) spectra of $P(ZnP)_{16}$ in the presence of various concentration of C_{60} to observe the structural change in $P(ZnP)_{16}$. The CD spectrum of a benzonitrile solution of $P(ZnP)_{16}$ (Fig. 5: blue line) shows cotton effect originating from the porphyrin Soret band at 428 nm. The intensity of the signal corresponding to the Soret band of $P(H_2P)_{16}$ decreases with increasing the concentration of C_{60}. This indicates that structures in $P(ZnP)_{16}$ are less ordered due to formation of the supramolecular complex between porphyrins and C_{60}.

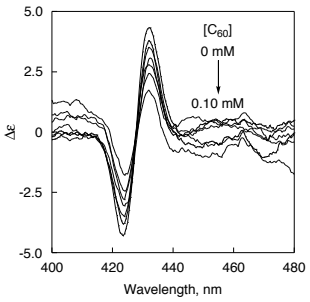

Fig. 5 Circular dichroism (CD) spectra of $P(ZnP)_{16}$ (6.1×10^{-6} M based on one porphyrin unit) in the presence of various concentration of C_{60} (0 to 1.0×10^{-4} M) in PhCN.

Electrophoretic deposition of $P(H_2P)_n$ [$P(ZnP)_n$] and C_{60} mixed clusters on OTE/SnO_2 electrode. Upon subjecting the resultant cluster suspension to a high electric dc field (500 V/cm for 1 min), mixed porphyrin-peptide oligomers [$P(H_2P)_n$ or $P(ZnP)_n$] and C_{60} clusters [$(P(H_2P)_n+C_{60})_m$ or $(P(ZnP)_n+C_{60})_m$] were deposited onto an optically transparent electrode (OTE) of a nanostructured SnO_2 electrode (OTE/SnO_2), to give modified electrodes [denoted as $(P(H_2P)_n+C_{60})_m$ or $(P(ZnP)_n+C_{60})_m$ (n = 1, 2, 4, 8, 16)]. The scanning electron micrograph (SEM) image of $(P(H_2P)_{16}+C_{60})_m$ deposited electrode reveals the cluster aggregation with a regular size (Fig. 6A). The $(P(H_2P)_{16}+C_{60})_m$ film on the electrode is composed of closely packed clusters of around 100 nm size. The cluster size in the SEM image is similar to that observed in the TEM image of the composite clusters prepared in acetonitrile/toluene (3/1, v/v) (Fig. 2A).

The absorptivity of the porphyrin-peptide oligomers-C_{60} composite films on ITO/SnO_2 electrodes $(P(ZnP)_{16}+C_{60})_m$, $(P(H_2P)_{16}+C_{60})_m$ and $(P(H_2P)_8+C_{60})_m$: spectra a-c in Fig. 6B) is much enhanced as compared with that of the reference system containing porphyrin unit alone [$(P(H_2P)_8)_m$]: spectrum d in Fig. 6B).[30,31] These results ensure that incident light is absorbed intensively in the visible and near-infrared regions by $(P(ZnP)_n+C_{60})_m$ and $(P(H_2P)_n+C_{60})_m$ due to the supramolecular π-complex formation between porphyrins and C_{60}.[33-35]

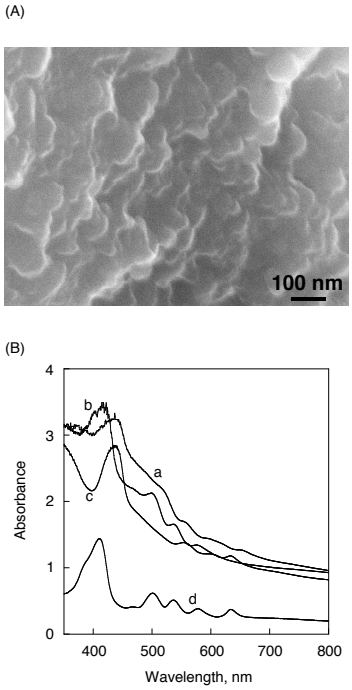

Fig. 6 (A) Scanning electron micrograph (SEM) image of $(P(H_2P)_{16}+C_{60})_m$. (B) Absorption spectra of OTE/SnO_2 modified with (a) $(P(H_2P)_{16}+C_{60})_m$, (b) $P(H_2P)_8+C_{60})_m$, (c) $P(ZnP)_{16}+C_{60})_m$ and (d) $(P(H_2P)_8)_m$ composite clusters.

Photocurrent generation properties. Photoelectrochemical measurements were performed with a standard two-electrode system consisting of a working electrode and a Pt wire gauze electrode in 0.5 M NaI and 0.01 M I_2 in air-saturated acetonitrile. We have previously reported that the incident photon-to-photocurrent efficiency (IPCE) increases with increasing C_{60} concentration (0 to 0.31 mM in acetonitrile/toluene) at a constant concentration of $P(H_2P)_8$ (0.024 mM).[28] This indicates that efficient electron-transfer from the excited state of porphyrin to C_{60} occurs, leading to efficient photocurrent generation.[30,31]

Fig. 7A shows the IPCE of the $(P(H_2P)_n+C_{60})_m$ (n = 1, 2, 4, 8, 16) modified electrode at a constant concentration ratio of porphyrin to C_{60} (*vide supra*). The IPCE value of $(P(H_2P)_n+C_{60})_m$ system exhibits a remarkable increase with increasing the number of porphyrins in a polypeptide unit. In particular, the $(P(H_2P)_{16}+C_{60})_m$ system has the maximum IPCE value of 48% at 600 nm as well as the broad photoresponse, extending into the infrared region up to 1000 nm. Such an effective light energy conversion is ascribed to the polypeptide structure to control three-dimensional organization between porphyrins and C_{60}. On the other hand, Fig. 7B shows the photocurrent action spectra of the $(P(ZnP)_n+C_{60})_m$ (n = 1, 2, 4, 8, 16) electrode at a constant concentration ratio of porphyrin to C_{60} (*vide supra*). The IPCE value of $(P(ZnP)_n+C_{60})_m$ modified electrodes also exhibits a remarkable increase with increasing number of porphyrin moieties in a polypeptide unit. The maximum IPCE of $(P(ZnP)_n+C_{60})_m$ system also exhibits a remarkable increase with increasing the number of porphyrins in a polypeptide unit. The

maximum IPCE of $(P(ZnP)_n+C_{60})_m$ is determined as 56% at 480 nm.

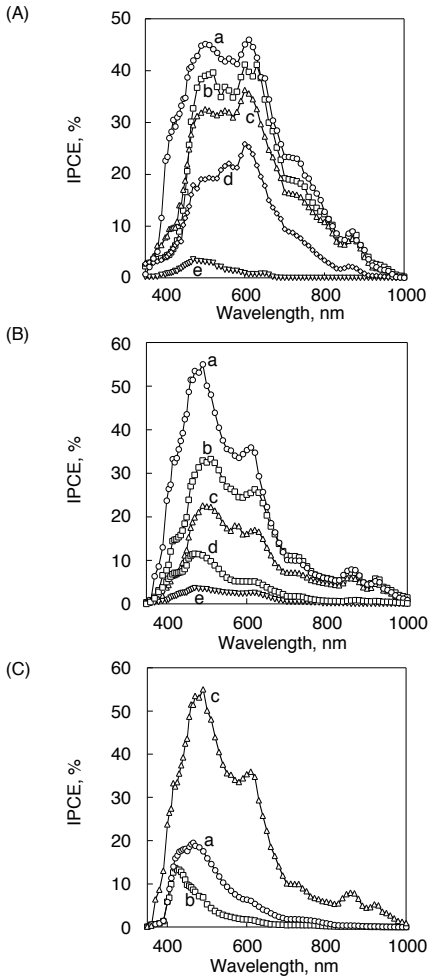

Fig. 7 (A) The photocurrent action spectra (IPCE *vs.* wavelength) of (a) $(P(H_2P)_{16}+C_{60})_m$, (b) $(P(H_2P)_8+C_{60})_m$, (c) $(P(H_2P)_4+C_{60})_m$, (d) $P(H_2P)_2+C_{60})_m$ and (e) $(P(H_2P)_1+C_{60})_m$ modified OTE/SnO_2 electrodes. (B) The photocurrent action spectra of (a) $(P(ZnP)_{16}+C_{60})_m$, (b) $(P(ZnP)_8+C_{60})_m$, (c) $(P(ZnP)_4+C_{60})_m$, (d) $(P(ZnP)_2+C_{60})$ and (e) $(P(ZnP)_1+C_{60})_m$ modified electrodes. (C) The photocurrent action spectra of (a) $(P(ZnP)_{16}+C_{60}Im)_m$, (b) $(P(ZnP)_{16}+C_{60}Py)_m$ and (c) $(P(ZnP)_{16}+C_{60})_m$ modified OTE/SnO_2 electrodes. See text for the employed concentration of the individual species.

Three important observations emerge from the comparison of IPCE photocurrent action spectra of $(P(ZnP)_n+C_{60})_m$ and $(P(H_2P)_n+C_{60})_m$ modified electrodes. First, IPCE values increase with increasing the number of porphyrins in a polypeptide unit in both $(P(H_2P)_n+C_{60})_m$ and $(P(ZnP)_n+C_{60})_m$ (n = 1, 2, 4, 8, 16) systems. This increase is indicative of the fact that efficient photoinduced electron-transfer occurs from excited state of the porphyrin unit to C_{60} in the supramolecular complex with increasing the number of porphyrins in a polypeptide unit (*vide supra*). This trend is in good agreement with the results of association constants between porphyrins and C_{60} based on absorption and fluorescence spectral changes (*vide supra*). Second observation is that the maximum IPCE value of $(P(ZnP)_{16}+C_{60})_m$ (56%) is greater than that of $(P(H_2P)_{16}+C_{60})_m$ (48%). This may be ascribed to driving force for photoinduced electron transfer or the energy level of triplet excited state of porphyrin (see: Scheme 2). The last observation concerns with the action spectra of $(P(H_2P)_n+C_{60})_m$ modified electrode which covers the region up to 950 nm and this response is broader than those of $(P(ZnP)_n+C_{60})_m$ modified electrode. This is further indicative of the stronger association between porphyrins and C_{60} in a polypeptide structure in $(P(H_2P)_n+C_{60})_m$.

We have also compared IPCE spectra of $(P(ZnP)_{16}+C_{60}Im)_m$ and $(P(ZnP)_{16}+C_{60}Py)_m$ modified electrodes with that of $(P(ZnP)_{16}+C_{60})_m$ in order to examine the effect of coordination bond of C_{60} derivatives on IPCE as shown in Fig. 7C. The maximum IPCE values of $(P(ZnP)_{16}+C_{60}Py)_m$ and $(P(ZnP)_{16}+C_{60}Im)_m$ are 20% and 15%, respectively. These values are much smaller than that of $(P(ZnP)_{16}+C_{60})_m$ (56%), whereas the binding constant of $P(ZnP)_{16}$-C_{60} is smaller than those of $P(ZnP)_{16}$-C_{60}Im and $P(ZnP)_{16}$-C_{60}Py (*vide supra*). This suggests that stronger interaction between porphyrin and C_{60} derivatives does not necessary improve the IPCE values. There are two essential factors in efficient photocurrent generation. One is the charge separation between porphyrin and fullerene, and the other is the resulting hole and electron transport in the thin film. Taking into consideration the large association constants in all the investigated systems [$P(ZnP)_{16}$-C_{60}, $P(ZnP)_{16}$-C_{60}Im, and $P(ZnP)_{16}$-C_{60}Py], a key element for efficient photocurrent generation is mainly the hole and electron transport in the thin film rather than the charge separation between porphyrins and C_{60}. The lower IPCE values of $P(ZnP)_{16}$-C_{60}Im and $P(ZnP)_{16}$-C_{60}Py systems as compared with that of $P(ZnP)_{16}$-C_{60} system may result from the poor electron transport properties of C_{60} derivatives due to the steric hindrance of the ligand moiety (Fig. 7C).

Power conversion efficiency. In order to examine the power conversion efficiency of porphyrin-peptide oligomer/C_{60} composite films, we have measured current-voltage (*I/V*) characteristics (Fig. 8). Fig. 8A shows *I/V* characteristics of (a) $(P(H_2P)_{16}+C_{60})_m$, (b) $(P(H_2P)_8+C_{60})_m$ and (c) $(P(H_2P)_1+C_{60})_m$ modified electrodes under visible light irradiation ($\lambda > 400$ nm), respectively. The $(P(H_2P)_{16}+C_{60})_m$ system has a larger fill factor (*FF*) of 0.47, an open circuit voltage (V_{oc}) of 320 mV, a short circuit current density (I_{sc}) of 0.36 mA cm^{-2}, and the overall power conversion efficiency (η) of 1.6% at input power (W_{in}) of 3.4 mW cm^{-2}.[37] The corresponding η values of $(P(H_2P)_8+C_{60})_m$ and $(P(H_2P)_1+C_{60})_m$ modified electrodes are 1.3% and 0.043%, respectively.[38] This order of increase in the η values largely agrees with the trend observed in IPCE experiments. The η values of $(P(H_2P)_{16}+C_{60})_m$ system is also remarkably enhanced (around 40 times) in comparison with the $(P(H_2P)_1+C_{60})_m$ modified electrode (η = 0.043%) under the same experimental conditions. The η value of $(P(ZnP)_{16}+C_{60})_m$ is also determined as 1.4% and this value is much larger than that of $(P(ZnP)_1+C_{60})_m$ (0.047%) as shown in Fig. 8B. These data of light energy conversion properties are summarized in table 2.

Fluorescence spectra and fluorescence lifetime measurements on OTE/SnO_2 surface. We have measured the fluorescence spectra on the OTE/SnO_2 surface to examine the quenching efficiency of porphyrins by C_{60} in $(P(H_2P)_n+C_{60})_m$

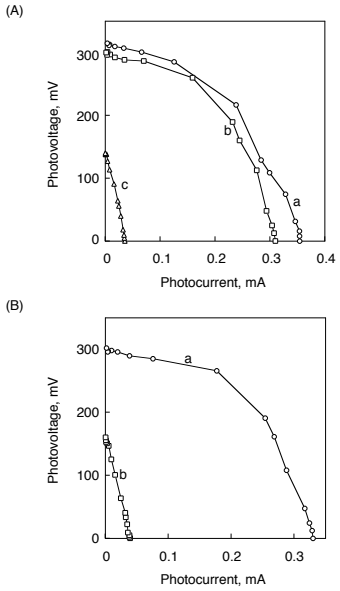

Fig. 8 (A) Current-voltage characteristics of (a) $(P(H_2P)_{16}+C_{60})_m$, (b) $(P(H_2P)_8+C_{60})_m$, and (c) $(P(H_2P)_1+C_{60})_m$ modified electrodes. (B) Current-voltage characteristics of (a) $(P(ZnP)_{16}+C_{60})_m$ and (b) $(P(ZnP)_1+C_{60})_m$. Electrolyte: 0.5 M NaI and 0.01 M I_2 in acetonitrile. Input power: 3.4 mW cm^{-2}, $\lambda > 400$ nm.

Table 2. Summary of photoelectrochemical data (IPCE and η).

System	IPCE (%)	η(%)	System	IPCE (%)	η(%)
$(P(ZnP)_1+C_{60})_m$	4	0.047	$(P(H_2P)_1+C_{60})_m$	4	0.043
$(P(ZnP)_2+C_{60})_m$	12		$(P(H_2P)_2+C_{60})_m$	26	
$(P(ZnP)_4+C_{60})_m$	22		$(P(H_2P)_4+C_{60})_m$	36	
$(P(ZnP)_8+C_{60})_m$	33		$(P(H_2P)_8+C_{60})_m$	42	1.3
$(P(ZnP)_{16}+C_{60})_m$	56	1.4	$(P(H_2P)_{16}+C_{60})_m$	48	1.6
$(P(ZnP)_{16}+C_{60}Im)_m$	15				
$(P(ZnP)_{16}+C_{60}Py)_m$	20				

systems. The fluorescence intensities of $(P(H_2P)_{16}+C_{60})_m$ are much smaller than that of the single component system of $(P(H_2P)_{16})_m$ on the electrode surface. This clearly indicates that the excited state of porphyrin is strongly quenched by photoinduced electron transfer to C_{60} in the supramolecular complex (Fig. 9A).[17-22]

The fluorescence lifetimes on the OTE/SnO_2 surface were also measured by time-correlated single photon counting technique at emission wavelengths of 650 nm for $(P(H_2P)_n)_m$ modified electrodes with excitation of the porphyrin moiety at 420 nm as shown in Fig. 9B. The decay curves of the fluorescence intensity could be fitted as three exponentials.

The fluorescence of $(P(H_2P)_n+C_{60})_m$ (n = 1, 2, 4, 8, 16) electrodes is significantly quenched as compared to the corresponding $(P(H_2P)_n)_m$ without C_{60}. This fluorescence quenching demonstrates the occurrence of ultrafast electron-transfer from the singlet excited states of porphyrins to C_{60} in the supramolecular complex (*vide infra*).[17-22]

The fluorescence lifetimes are listed in Table 3. The fluorescence lifetimes of $(P(H_2P)_n)_m$ on the electrode surface decrease with increasing the number of porphyrins in a polypeptide unit. This supports the increasing interaction

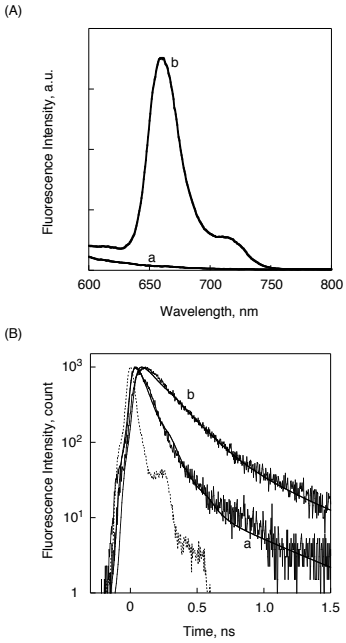

Fig. 9 (A) Fluorescence spectra of (a) $(P(H_2P)_{16}+C_{60})_m$ and (b) $(P(H_2P)_{16})_m$ on OTE/SnO_2 surface. λ_{ex} = 420 nm. (B) Fluorescence decay curves of (a) $(P(H_2P)_{16}+C_{60})_m$ and (b) $(P(H_2P)_{16})_m$ modified electrodes. The fluorescence decays are observed at 650 nm by the time-correlated single-photon counting method. The fluorescence intensities are normalized for comparison. The excitation wavelength is 420 nm and IRF (instrument response function) curves are presented for each decay.

Table 3. Fluorescence lifetime (τ) of the composite films

System	τ_1	τ_2	τ_3
$(P(H_2P)_1)_m$	220 ps (60.6%)	639 ps (33.5%)	3.0 ns (5.9%)
$(P(H_2P)_2)_m$	200 ps (67.2%)	502 ps (29.4%)	2.5 ns (3.4%)
$(P(H_2P)_4)_m$	183 ps (76.6%)	498 ps (21.6%)	2.4 ns (1.8%)
$(P(H_2P)_8)_m$	164 ps (78.4%)	507 ps (20.5%)	1.7 ns (1.1%)
$(P(H_2P)_{16})_m$	166 ps (91.8%)	593 ps (8.2%)	
$(P(ZnP)_1)_m$	57 ps (97.4%)	553 ps (2.6%)	
$(P(ZnP)_8)_m$	48 ps (100%)		
$(P(ZnP)_{16})_m$	35 ps (100%)		
$(P(H_2P)_1+C_{60})_m$	135 ps (71.6%)	518 ps (33.5%)	2.2 ns (3.0%)
$(P(H_2P)_2+C_{60})_m$	129 ps (83.0%)	469 ps (15.7%)	2.2 ns (1.3%)
$(P(H_2P)_4+C_{60})_m$	64 ps (95.5%)	500 ps (15.7%)	3.8 ns (0.5%)
$(P(H_2P)_8+C_{60})_m$	24 ps (99.6%)	482 ps (0.4%)	
$(P(H_2P)_{16}+C_{60})_m$	70 ps (98.8%)	482 ps (1.2%)	
$(P(ZnP)_1+C_{60})_m$	58 ps (96.7%)	621 ps (3.3%)	
$(P(ZnP)_8+C_{60})_m$	25 ps (100%)		
$(P(ZnP)_{16}+C_{60})_m$	16 ps (100%)		

between the porphyrin moieties in a polypeptide unit. The multiple and decrease of lifetime components on the films may be because of strong interactions between porphyrins or from porphyrin to SnO_2 electrode in contrast with the single component and similar lifetime in toluene.[28] The fluorescence lifetimes of major component (τ_1) of $(P(H_2P)_n+C_{60})_m$ are clearly smaller than those of $(P(H_2P)_n)_m$ without C_{60} and decrease with increasing the number of porphyrins in a polypeptide unit (Table

3), although the similar multiple components are observed. This trend may arise from the change in the driving force of electron transfer because of the strong supramolecular formation between porphyrins and C_{60}, which leads to acceleration of the charge-separated state. This agrees with enhancement of the IPCE values with increasing the number of porphyrins in a polypeptide unit (Fig. 7A). On the modified electrodes, he τ_1 values of $(P(ZnP)_n+C_{60})_m$ (n = 8, 16) are also smaller than those of $(P(ZnP)_n)_m$ (n = 8, 16) without C_{60} as the case of the $(P(H_2P)_n+C_{60})_m$. Additionally, the τ_1 value of $(P(ZnP)_{16}+C_{60})_m$ is much smaller than those of $(P(ZnP)_n+C_{60})_m$ (n = 1, 8). Thus, the supramolecular complex formation between porphyrins and C_{60} becomes more favored with increasing the number of porphyrin in a polypeptide unit to facilitate photoinduced electron transfer from the singlet excited state of porphyrin to C_{60}, leading to an efficient photocurrent generation.

Electron spin resonance (ESR) measurement. The formation of the radical cation of $P(ZnP)_{16}$ and the radical anion of C_{60} in $(P(ZnP)_{16}+C_{60})_m$ composite clusters upon photoexcitation is confirmed by the electron spin resonance (ESR) measurements performed in frozen acetonitrile/toluene under photoirradiation. The resulting ESR spectrum of $(P(ZnP)_{16}+C_{60})_m$ upon photoirradiation in acetonitrile/toluene at 123 K is shown in Fig. 10. The ESR signal (g = 2.002) is assigned to the overlap of two signals due to porphyrin radical cation and $C_{60}^{\bullet-}$.[39]

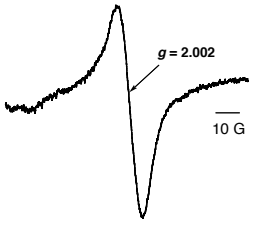

Fig. 10 ESR spectrum of photoirradiated $(P(ZnP)_{16}+C_{60})_m$ ([ZnP] = 0.012 mM; $[C_{60}]$ = 0.31 mM) in acetonitrile/toluene (3/1, v/v) under photoirradiation of a high-pressure mercury lamp, measured at 123 K.

Femtosecond transient absorption spectra of composite clusters. The photodynamics of the composite molecular clusters of zinc porphyrins with a polypeptide unit $[P(ZnP)_n]$ and C_{60} was examined by the femtosecond time-resolved transient absorption spectra. The time-resolved transient absorption spectra of $(P(ZnP)_1+C_{60})_m$ in acetonitrile/toluene (3/1, v/v) are shown in Fig. 11A. Upon 387 nm laser pulse excitation we observe a broad absorption in the 450-510 nm as we populate the porphyrin singlet excited state. This transient quickly decays to form triplet excited state. The singlet and triplet excited state of porphyrins have been characterized earlier.[40] In addition, a strong transient bleaching (around 610 nm) arises from the fluorescence. Although the dominant triplet absorption of the porphyrin that overlaps with the absorption due to the charge-separated state has precludes the clear detection of the charge-separated state, fullerene radical anion generated by the photoinduced electron transfer is clearly detected in the nanosecond laser flash photolysis measurement (Fig. S2 in Supporting Information). The decay curve at 1070 nm due to $C_{60}^{\bullet-}$ can be well fitted by first-order kinetics rather than bimolecular second-order kinetics and the apparent lifetime of the back electron transfer is determined as 79 μs at 298 K.

In contrast to $(P(ZnP)_1+C_{60})_m$ system, the strong absorption arising from singlet and triplet excited states of porphyrins (450-510 nm) is missing in the case of $(P(ZnP)_8+C_{60})_m$ and $(P(ZnP)_{16}+C_{60})_m$. Instead a broad absorption at around 650 nm appears after the laser pulse excitation as shown in Fig. 11B and C. The transient absorption spectra of $(P(H_2P)_{16}+C_{60})_m$ exhibit the similar trend to the $(P(ZnP)_{16}+C_{60})_m$; see Fig.11D. Such broad absorption spectra are clear indication of formation of the porphyrin radical cation.[41] It is also interesting to note that the bleaching originating from fluorescence (610 nm region) is absent in the transient spectra (Fig. 11B and C).

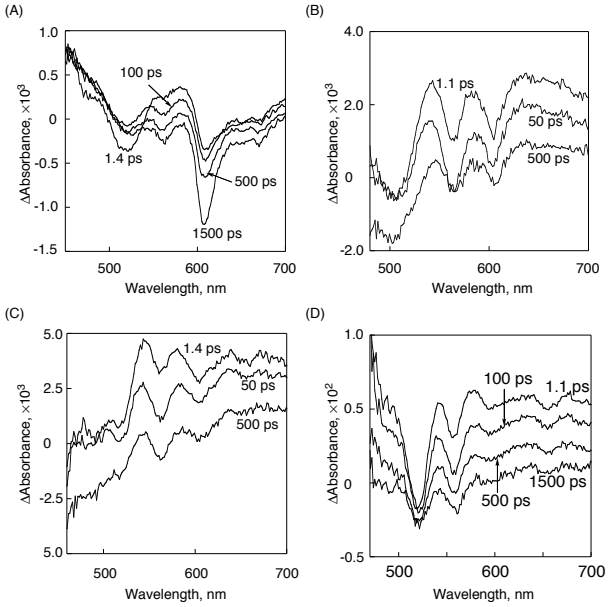

Fig. 11 Time-resolved absorption spectra recorded following 387 nm laser pulse excitation of (A) $(P(ZnP)_1+C_{60})_m$ ($[P(ZnP)_1]$ = 0.19 mM; $[C_{60}]$ = 0.31 mM). (B) $(P(ZnP)_8+C_{60})_m$ ($[P(ZnP)_8]$ = 0.024 mM; $[C_{60}]$ = 0.31 mM). (C) $(P(ZnP)_{16}+C_{60})_m$ ($[P(ZnP)_{16}]$ = 0.012 mM; $[C_{60}]$ = 0.31 mM). (D) $(P(H_2P)_{16}+C_{60})_m$ ($[P(H_2P)_{16}]$ = 0.012 mM; $[C_{60}]$ = 0.31 mM). All samples were prepared in argon-saturated acetonitrile/toluene (3/1, v/v) and measurements were made at 298 K.

These spectral features indicate that electron transfer from the singlet excited state of porphyrins to C_{60} occurs in the stronger supramolecular complex of $(P(ZnP)_8+C_{60})_m$ and $(P(ZnP)_{16}+C_{60})_m$ as compared to the corresponding monomer system (vide supra). Thus, photoinduced electron transfer from the singlet excited state of $P(ZnP)_n$ to C_{60} occurs in the composite clusters of $(P(ZnP)_n+C_{60})_m$ (n = 8, 16). Taking into consideration the same number of porphyrins in a polypeptide unit, the difference in the excited state interaction results from the organization of porphyrins and fullerenes. This behavior demonstrates that the organized assembly within a polypeptide unit facilitates the photoinduced electron transfer by forming the supramolecular complex. This trend is also in good agreement with the associate constant, fluorescence lifetime and IPCE results.

Photocurrent generation mechanism. Photocurrent generation in the present system is initiated by photoinduced charge separation from the singlet excited state of free base porphyrin ($^1H_2P^*/H_2P^+$ = -0.7 V vs NHE)[30] or zinc porphyrin ($^1ZnP^*/ZnP^+$ = -1.0 V vs NHE)[42] in the porphyrin-peptide oligomer to C_{60} (C_{60}/C_{60}^- = -0.2 V vs NHE)[30] in the porphyrin-C_{60} complex rather than direct electron injection to conduction band of SnO_2 (0 V vs NHE) system.[30] The reduced C_{60} injects electrons into the SnO_2 nanocrystallites, whereas the oxidized porphyrin ($H_2P/H_2P^{\cdot+}$ = 1.2 V or ZnP/ZnP^+ = 1.0 V vs NHE)[18b,30.31] undergoes the electron-transfer reduction with the iodide (I_3^-/I^- = 0.5 V vs NHE)[30] in the electrolyte system. The driving force of electron-transfer from $^1ZnP^*$ to C_{60} (0.8 eV) is significantly larger than that of electron transfer from $^1H_2P^*$ to C_{60} (0.5 eV). The larger IPCE value of $(P(ZnP)_{16}+C_{60})_m$ (56%) that that of $(P(H_2P)_{16}+C_{60})_m$ (48%) may be ascribed to the difference in the driving force of electron transfer. The increase in number of the porphyrin unit in porphyrin polypeptides results in formation of well-organized clusters as shown in Fig. 2 (B *vs* D). In such a case, electron injection following the charge separation occurs more effectively to a nanostructured SnO_2 electrode, which may arise from the increase of the surface area of the composite clusters, as revealed by the photoelectrochemical measurements (Fig. 7).

Scheme 2. Schematic illustration of photocurrent generation mechanism

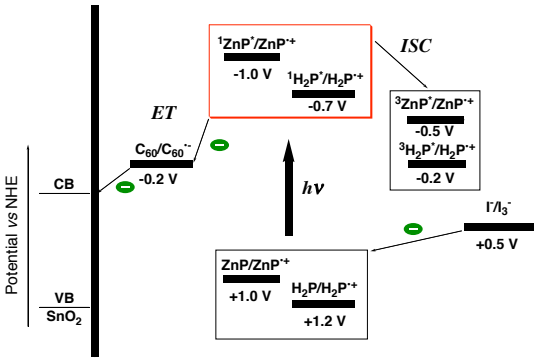

Conclusions

We have successfully constructed novel organic photovoltaic systems using supramolecular complexes of porphyrin-peptide oligomers with fullerene clusters. The highly colored composite clusters of porphyrin-peptide oligomers and fullerenes have been assembled as three-dimensional arrays onto nanostructured SnO_2 films using an electrophoretic deposition method. The composite cluster OTE/SnO_2 electrode prepared with an assembly of 16 porphyrin unit-polypeptide chain and C_{60} viz., $(P(ZnP)_{16}+C_{60})_m$ exhibits an impressive incident photon-to-photocurrent efficiency (IPCE) with values reaching as high as 56%. The broad photocurrent action spectra (with photoresponse extending up to 1000 nm) show the ability of these composites to harvest photons in the visible and infrared. The power conversion efficiency (η) of $(P(H_2P)_{16}+C_{60})_m$ modified electrode reaches 1.6%, which is 40 times higher than the value (0.043%) of the porphyrin monomer $(P(H_2P)_1+C_{60})_m$ modified electrode. Thus, organization approach between porphyrins and fullerenes with polypeptide structures is promising, and may make it possible to further improve the light energy conversion properties by using larger number of porphyrins in a polypeptide unit. Such an increase in the light energy conversion efficiency is ascribed to the enhancement of photoinduced electron-transfer in the supramolecular assembly.

Acknowledgements

This work was partially supported by a Grant–in–Aid from the Ministry of Education, Culture, Sports, Science and Technology, Japan. PVK acknowledges the support from the Office of Basic Energy Science of the U. S. Department of the Energy. This is contribution No. NDRL 4680 from the Notre Dame Radiation Laboratory and from Osaka University. The work at Yonsei University has been supported by the Star Faculty Program of the Ministry of Education and Human Resources.

References

1 (a) B. O'Regan and M. Grätzel, *Nature* 1991, **353**, 737; (b) P. Bonhôte, J.-E. Moser, R. Humphry-Baker, N. Vlachopoulos, S. M. Zakeeruddin, L. Walder and M. Grätzel, *J. Am. Chem. Soc.* 1999, **121**, 1324; (c) U. Bach, D. Lupo, P. Comte, J. E. Moser, F. Weissörtel, J. Salbeck, H. Spreitzer and M. Grätzel, *Nature* 1998, **395**, 583.

2 (a) M. Grätzel, *Inorg. Chem.* 2005**, 44**, 6841; M. Grätzel, *Nature* 2001, **414**, 338; (b) A. Hagfeldt and M. Grätzel, *Chem. Rev.* 1995, **95**, 49.

3 (a) J. Xue, B. P. Rand, S. Uchida and S. R. Forrest, *J. Appl. Phys.* 2005, **98**, 124903; (b) J. G. Xue, S. Uchida, B. P. Rand and S. R. Forrest, *Appl. Phys. Lett.* 2004, **84**, 3013; (c) J. G. Xue, S. Uchida, B. P. Rand and S. R. Forrest, *Appl. Phys. Lett.* 2004, **85**, 5757; (d) P. V. Kamat, *J. Phys. Chem. C* 2007, **111**, 2834.

4 (a) A. Shah, P. Torres, R. Tscharner, N. Wyrsch and H. Keppner, *Science* 1999, **285**, 69; (b) J. J. M. Halls, C. A. Walsh, N. C. Greenham, E. A. Marseglia, R. H. Friend, S. C. Moratti and A. B. Holmes, *Nature* 1995, **376**, 498; (c) L. Schmidt-Mende, A. Fechtenkötter, K. Müllen, E. Moons, R. H. Friend and J. D. MacKenzie, *Science* 2001, **293**, 1119; (d) J. J. M. Halls, C. A. Walsh, N. C. Greenham, E. A. Marseglia, R. H. Friend, S. C. Moratti and A. B. Holmes, *Nature* 1995, **376**, 498; (e) W. L. Ma, C. Y. Yang, X. Gong, K. Lee and A. J. Heeger, *Adv. Funct. Mater.* 2005, **15**, 1617; (f) W. U. Huynh, J. J. Dittmer and A. P. Alivisatos, *Science* 2002, **295**, 2425.

5 (a) X. Yang, J. Loos, S. C. Veenstra, W. J. H. Verhees, M. M. Wienk, J. M. Kroon, M. A. J. Michels and R. A. J. Janssen, *Nano Lett.* 2005 **5**, 579; (b) M. M. Wienk, J. M. Kroon, W. J. H. Verhees, J. Knol, J. C. Hummelen, P. A. van Hal and R. A. J. Janssen, *Angew. Chem. Int. Ed.* 2003, **42**, 3371.

6 (a) S. E. Shaheen, C. J. Brabec, N. S. Sariciftci, F. Padinger, T. Fromherz and J. C. Hummelen, *Appl. Phys. Lett.* 2001, **78**, 841; (b) F. Padinger, R. S. Rittberger and N. S. Sariciftci, *Adv. Funct. Mater.* 2003, **13**, 85; (c) C. Brabec, *Sol. Energy Mater. Sol. Cells* 2004, **83**, 273; (d) C. J. Brabec, N. S. Sariciftci and J. C. Hummelen, *Adv. Funct. Mater.* 2001, **11**, 15; (e) In *Organic Photovoltaics*, ed. S.-S. Sun and N. S. Sariciftci, Taylor & Francis, Boca Raton, 2005.

7 (a) G. Yu, J. Gao, J. C. Hummelen, F. Wudl and A. J. Heeger, *Science* 1995, **270**, 1789; (b) S. Khodabakhsh, B. M. Sanderson, J. Nelson and T. S. Jones, *Adv. Funct. Mater.* 2006, **16**, 95.

8 (a) *The Photosynthetic Reaction Center*, ed. J. Deisenhofer and J. R. Norris, Academic Press, San Diego, 1993; (b) *Anoxygenic*

Photosynthetic Bacteria, ed. R. E. Blankenship, M. T. Madigan and C. E. Bauer, Kluwer Academic Publishing, Dordrecht, 1995.

9 R. J. Cogdell and J. G. Lindsay, *TIBTECH*, 1998, **16**, 521.

10 (a) G. McDermott, S. M. Prince, A. A. Freer, A. M. Hawthornthwaite-Lawless, M. Z. Papiz, R. J. Cogdell and N. W. Isaacs, *Nature* 1995, **374**, 517; (b) J. Koepke, X. Hu, C. Muenke, K. Schulten and H. Michel, *Structure* 1996, **4**, 581.

11 S. G. Boxer, *Annu. Rev. Biophys. Bioeng.* 1990, **19**, 267.

12 (a) S. Fukuzumi, in *The Porphyrin Handbook*, ed. K. M. Kadish, K. M. Smith and R. Guilard, Academic Press, San Diego, 2000, vol. 8, pp. 115–152; (b) S. Fukuzumi, Y. Endo and H. Imahori, *J. Am. Chem. Soc.* 2002, **124**, 10974.

13 (a) S. Karrasch, P. A. Bullough and R. Ghosh, *EMBO J.* 1995, **14**, 631; (b) H. Savage, M. Cyrklaff, G. Montoya, W. Kuhlbrandt and I. Sinning, *Structure* 1996, **4**, 243; (c) T. Walz, S. J. Jamieson, C. M. Bowers, P. A. Bullough and C. N. Hunter, *J. Mol. Biol.* 1998, **282**, 833.

14 (a) J. K. M. Sanders, in *Comprehensive Supramolecular Chemistry*, ed. J. L. Atwood, J. E. D. Davies, D. D. MacNicol and F. Vogtle, Pergamon Press, Oxford, 1996, vol. 9, pp. 131–164; J. K. M. Sanders, in *The Porphyrin Handbook*, ed. K. M. Kadish, K. M. Smith and R. Guilard, Academic Press, New York, 2000, vol. 3, pp. 347–368; (b) J. Li, A. Ambroise, S. I. Yang, J. R. Diers, J. Seth, C. R. Wack, D. F. Bocian, D. Holten and J. S. Lindsey, *J. Am. Chem. Soc.* 1999, **121**, 8927; (c) O. Mongin, A. Schuwey, M.-A. Vallot and A. Gossauer, *Tetrahedron Lett.* 1999, **40**, 8347.

15 (a) J. Barber and B. Andersson, *Nature* 1994, **370**, 31; W. Kuéhlbrandt, *Nature* 1995, **374**, 497; (b) T. Pullerits and V. Sundström, *Acc. Chem. Res.* 1996, **29**, 381.

16 N. Solladié, A. Hamel and M. Gross, *Tetrahedron Lett.* 2000, **41**, 6075.

17 (a) S. Fukuzumi and H. Imahori, in *Electron Transfer in Chemistry*, ed. V. Balzani, Wiley-VCH, Weinheim, 2001, vol. 2, pp. 927–975; (b) S. Fukuzumi and D. M. Guldi, in *Electron Transfer in Chemistry*, ed. V. Balzani, Wiley-VCH, Weinheim 2001, vo. 2, pp. 270–337.

18 (a) H. Imahori, K. Tamaki, D. M. Guldi, C. Luo, M. Fujitsuka, O. Ito, Y. Sakata and S. Fukuzumi, *J. Am. Chem. Soc.* 2001, **123**, 2607; (b) H. Imahori, D. M. Guldi, K. Tamaki, Y. Yoshida, C. Luo, Y. Sakata and S. Fukuzumi, *J. Am. Chem. Soc.* 2001, **123**, 6617; (c) H. Imahori, H. Yamada, D. M. Guldi, Y. Endo, A. Shimomura, S. Kundu, K. Yamada, T. Okada, Y. Sakata and S. Fukuzumi, *Angew. Chem. Int. Ed.* 2002, **41**, 2344; (d) H. Imahori, K. Tamaki, Y. Araki, Y. Sekiguchi, O. Ito, Y. Sakata and S. Fukuzumi, *J. Am. Chem. Soc.* 2002, **124**, 5165; (e) C. Luo, D.M. Guldi, H. Imahori, K. Tamaki and Y. Sakata, *J. Am. Chem. Soc.* 2000, **122**, 6535.

19 (a) S. Fukuzumi, *Pure Appl. Chem.* 2003, **75**, 577; (b) S. Fukuzumi, *Org. Biomol. Chem.* 2003, **1**, 609; (c) S. Fukuzumi, *Bull. Chem. Soc. Jpn*. 2006, **79**, 177.

20 M. R. Wasielewski, *Chem. Rev.* 1992, **92**, 435.

21 (a) D. Gust, T. A. Moore and A. L. Moore, *Acc. Chem. Res*. 1993, **26**, 198; (b) D. Gust, T. A. Moore and A. L. Moore, *Acc. Chem. Res.* 2001, **34**, 40; (c) D. Gust and T. A. Moore, in *The Porphyrin Handbook*, ed. K. M., Kadish, K. M., Smith and R. Guilard, Academic Press, San Diego, CA, 2000, vol. 8, pp. 153–190.

22 (a) M.-S. Choi, T. Aida, H. Luo, Y. Araki and O. Ito, *Angew. Chem. Int. Ed.* 2003, **42**, 4060; (b) K. Li, D. I. Schuster, D. M. Guldi, M. A. Herranz and L. Echegoyen, *J. Am. Chem. Soc.* 2004, **126**, 3388; (c) F. D'Souza, G. R. Deviprasad, M. E. El-Khouly, M. Fujitsuka and O. Ito, *J. Am. Chem. Soc.* 2001, **123**, 5277; (d) N. Armaroli, G. Marconi, L. Echegoyen, J.-P. Bourgeois and F. Diederich, *Chem. Eur. J.* 2000, **6**, 1629; (e) F. D'Souza, P. M. Smith, M. E. Zandler, A. L. McCarty, M. Itou, Y. Araki and O. Ito, *J. Am. Chem. Soc.* 2004, **126**, 7898.

23 F. Diederich and M. Gömez-Löpez, *Chem. Soc. Rev.* 1999, **28**, 263.

24 (a) P. D. W. Boyd, M. C. Hodgson, C. E. F. Rickard, A. G. Oliver, L. Chaker, P. J. Brothers, R. D. Bolskar, F. S. Tham and C. A. Reed, *J. Am. Chem. Soc*. 1999, **121**, 10487; (b) D. Sun, F. S. Tham, C. A. Reed, and P. D. W. Boyd, *Proc. Natl. Acad. Sci. U.S.A.* 2002, **99**, 5088; (c) D. Sun, F. S. Tham, C. A. Reed, L. Chaker and P. D. W. Boyd, *J. Am. Chem. Soc.* 2002, **124**, 6604; (d) P. D. W. Boyd and C. A. Reed, *Acc. Chem. Res.* 2005, **38**, 235; (e) A. Hosseini, M. C. Hodgson, F. S. Tham, C. A. Reed and P. D. W. Boyd, *Cryst. Growth Des.* 2006, **6**, 397.

25 (a) M. M. Olmstead, D. A. Costa, K. Maitra, B. C. Noll, S. L. Phillips, P. M. Van Calcar and A. L. Balch, *J. Am. Chem. Soc*. 1999, **121**, 7090; (b) M. M. Olmstead, A. de Bettencourt-Dias, J. C. Duchamp, S. Stevenson, D. Marciu, H. C. Dorn and A. L. Balch, *Angew. Chem. Int. Ed***.** 2001, **40**, 1223; (c) H. M. Lee, M. M. Olmstead, G. G. Gross and A. L. Balch, *Cryst. Growth Des.* 2003**, 3** 691.

26 (a) K. Tashiro, T. Aida, J.-Y. Zheng, K. Kinbara, K. Saigo, S. Sakamoto and K. Yamaguchi, *J. Am. Chem. Soc*. 1999, **121**, 9477; (b) J.-Y. Zheng, K. Tashiro, Y. Hirabayashi, K. Kinbara, K. Saigo, T. Aida, S. Sakamoto and K. Yamaguchi, *Angew. Chem. Int. Ed.* 2001, **40**, 1857.

27 Y.-B. Wang and Z. Lin, *J. Am. Chem. Soc*. 2003, **125**, 6072.

28 A preliminary report: T. Hasobe, P. V. Kamat, V. Troiani, N. Solladie, T. K. Ahn, S. K. Kim, D. Kim, A. Kongkanand, S. Kuwabata and S. Fukuzumi, *J. Phys. Chem. B.* 2005, **109**, 19.

29 I. Bedja, S. Hotchandani and P. V. Kamat, *J. Phys. Chem.* 1994, **98**, 4133.

30 (a) T. Hasobe, H. Imahori, S. Fukuzumi and P. V. Kamat, *J. Mater. Chem.* 2003, **13**, 2515; (b) T. Hasobe, H. Imahori, S. Fukuzumi and P. V. Kamat, *J. Phys. Chem. B* 2003, **107**, 12105.

31 T. Hasobe, H. Imahori, P. V. Kamat, T. K. Ahn, S. K. Kim, D. Kim, A. Fujimoto, T. Hirakawa and S. Fukuzumi, *J. Am. Chem. Soc.* 2005, **127**, 1216.

32 (a) H. Imahori, N. V. Tkachenko, V. Vehmanen, K. Tamaki, H. Lemmetyinen, Y. Sakata and S. Fukuzumi, *J. Phys. Chem. A* 2001, **105**, 1750; (b) N. V. Tkachenko, C. Guenther, H. Imahori, K. Tamaki, Y. Sakata, S. Fukuzumi and H. Lemmetyinen, *Chem. Phys. Lett.* 2000, **326**, 344.

33 N. V. Tkachenko, H. Lemmetyinen, J. Sonoda, K. Ohkubo, T. Sato, H. Imahori and S. Fukuzumi, *J. Phys. Chem. A.* 2003, **107**, 8834.

34 (a) F. D'Souza, S. Gadde, M. E. Zandler, K. Arkady, M. E. El-Khouly, M. Fujitsuka and O. Ito, *J. Phys. Chem. A* 2002, **106**, 12393; (b) D. I. Schuster, P. D. Jarowski, A. N. Kirschner and S. R. Wilson, *J. Mater. Chem.* 2002, **12**, 2041.

35 (a) N. V. Tkachenko, L. Rantala, A. Y. Tauber, J. Helaja, P. H. Hynninen and H. Lemmetyinen, *J. Am. Chem. Soc.* 1999, **121**, 9378; (b) N. Armaroli, G. Marconi, L. Echegoyen, J.-P. Bourgeois and F. Diederich, *Chem. Eur. J.* 2000, **6**, 1629.

36 H. A. Benesi and J. H. Hildebrand, *J. Am. Chem. Soc.* 1949, **71**, 2703.

37 The η value of OTE/SnO_2/$(P(H_2P)_{16}+C_{60})_m$ system is ~0.7% at input power (W_{in}) of 100 mW cm^{-2}.

38 The prompt, steady and reproducible photocurrent and photovoltage responses upon the excitation of OTE/SnO_2/$(P(H_2P)_8+C_{60})_m$ electrode in the visible region (λ > 400 nm) are shown in Fig. S1A and S1B, respectively (see Supporting Information).

39 A strong interaction with porphyrins lowers the symmetry of $C_{60}^{\bullet-}$, resulting in an increase in the *g* value. This may be the reason why the two signals are overlapped; see: S. Fukuzumi, H. Mori, T. Suenobu, H. Imahori, X. Gao and K. M. Kadish, *J. Phys. Chem. A* 2000, **104**, 10688.

40 R. Bonnett, D. J. McGarvey, A. Harriman, E. J. Land, T. G. Truscott and U.-J. Winfield, *Photochem. Photobiol.* 1988, **48**, 271.

41 Z. Gasyna, W. R. Browett and M. J. Stillman, *Inorg. Chem.* 1985, **24**, 2440.

42 The one-electron oxidation potential of ZnP was determined as ~1.0 V (vs NHE). The excitation energy of the singlet and triplet excited states were also calculated as ~2.0 and 1.5 eV, respectively.[18b]

Table of Content

Organic Solar Cells. Supramolecular Composites of Porphyrins and Fullerenes Organized by Polypeptide Structures as Light Harvesters

Taku Hasobe,* Kenji Saito, Prashant V. Kamat,* Vincent Troiani, Hongjin Qiu, Nathalie Solladié,* Kil Suk Kim, Jong Kang Park, Dongho Kim,* Francis D'Souza,* and Shunichi Fukuzumi*

Solar cells capable of incident photon-to-current conversion efficiency of up to 56% were constructed using a series of porphyrin-peptide oligomers and fullerene assembled on a nanostructured SnO_2 electrode using an electrophoretic deposition technique.

Needs a figure